Phi: Jurnal Pendidikan Fisika dan Terapan
Vol. 13, No. 1 (2027) 64-77
ISSN: 2460-4348, e-ISSN: 2549-7162
https://jurnal.ar-raniry.ac.id/index.php/jurnalphi/index

Article Type: *original research*

Mapping Shallow Zones with Potential for Land Subsidence Around Subsurface Water Channels Using 2D Electrical Resistivity Tomography in Bandung

Rio Restu Putra[1], Risky Martin Antosia[1], Wahyu Eko Junian[1*], Acep Ruchimat[2]
[1]Department of Geophysical Engineering, Faculty of Industrial Technology, Sumatra Institute of Technology, South Lampung, Indonesia
[2]Center for Groundwater and Environmental Geology, 57 Diponegoro Street, Bandung, West Java, Indonesia

Correspondence E-mail: wahyu.junian@tg.itera.ac.id

ARTICLE INFO

Article History:
Received: 04 May 2026
Revised: 29 July 2026
Accepted: 01 August 2026
Published: 08 September 2026

Keywords:
Electrical resistivity tomography (ERT); Land subsidence; Geotechnical investigation; Geohazard mitigation; Groundwater channel.

ABSTRACT

Recurring ground subsidence around the Cikapayang River, particularly near the Bandung Center for Groundwater and Environmental Geology (PATGTL), indicates ongoing subsurface instability despite previous remediation efforts. This phenomenon is associated with backfill soil, rainwater infiltration, and subsurface drainage structures that can reduce soil bearing capacity and promote the formation of weak zones and voids. This study aims to identify shallow subsurface conditions associated with recurring ground subsidence and potential weak zones around subsurface drainage structures. 2D Electrical Resistivity Tomography (ERT) using the Wenner–Schlumberger configuration was conducted along five survey lines, each 52 m long with a 1 m electrode spacing. The data were processed using Res2DInv, integrated and visualized in Leapfrog Geo, and validated through synthetic forward modeling using Res2DMod. Resistivity values ranged from 4.86 to 339 Ωm. The low-resistivity zone (4–30 Ωm) was interpreted as a water-saturated clay fill layer with low bearing capacity, while the high-resistivity zone (>101 Ωm) was associated with voids and subsurface drainage structures. Land subsidence zones were identified in four sections in the central area, while potential new land subsidence zones were detected at a depth of approximately 1 m in the outermost section. The results indicate that integrating ERT, synthetic modeling, and line merging is effective in identifying land subsidence-prone zones and supporting urban risk mitigation.

This work is licensed under a Creative Commons Attribution-ShareAlike 4.0 International License

1. INTRODUCTION

Land subsidence, as a geological issue, can occur naturally or be caused by human activities (Rizqi and Yudhana, 2021). Additionally, land subsidence may occur in areas underlain by weak or poorly compacted surface soils. Soil with these characteristics generally cannot retain large amounts of rainwater, allowing water to infiltrate into the subsurface and increasing the susceptibility to ground settlement, especially during periods of intense rainfall. This situation may become more

severe if the drainage system is not functioning properly or if there are changes in land use in the surrounding area.

This study was conducted in the vicinity of the Groundwater and Environmental Geology Headquarters (PATGTL), located near the Cikapayang River. The study site was selected because the area has experienced recurring ground subsidence. These subsidence events have caused underground water channels to become visible at the ground surface due to the collapse of their walls or frameworks. These conditions indicate soil stability issues that require further investigation. The ground subsidence observed at the study site is the second occurrence in the same area; the first event was recorded in 2012 and was repaired, but it reoccurred in 2025 in a different section, closer to the fence. This recurring event is strongly suspected to be related to the condition of the topsoil, which consists of fill soil. Fill soil generally has a less compact structure and relatively high porosity, making it less capable of withstanding rainwater infiltration (Zhao et al., 2022). During heavy rainfall, infiltrating water tends to flow toward subsurface drainage channels, potentially damaging the channels' framework and reducing the bearing capacity of the surrounding soil. This process can generate localized voids, weakened zones, and shallow ground instability that may eventually lead to land subsidence. Therefore, investigating the shallow subsurface conditions around these drainage channels is essential for understanding the mechanisms that trigger subsidence.

Several geophysical and remote sensing methods have been applied to investigate land subsidence phenomena. The time-lapse microgravity method can detect changes in subsurface mass distribution associated with compaction processes by measuring temporal variations in gravitational acceleration (Wahyudi et al. 2021). However, the method is generally more sensitive to large-scale mass changes and deeper subsurface structures, making it less effective for delineating small, shallow features such as localized weak zones or damaged subsurface drainage channels. Meanwhile, Differential Interferometric Synthetic Aperture Radar (DinSAR) utilizes phase differences between repeated Sentinel-1 radar acquisitions to monitor surface deformation with millimeter-scale accuracy (Widada et al. 2020). Although DinSAR is highly effective for mapping spatial and temporal patterns of subsidence at the ground surface, it does not directly provide information about the subsurface conditions responsible for the observed deformation. Previous resistivity studies have demonstrated the capability of electrical methods to identify weathered zones, fractures, cavities, and shallow weak zones related to subsidence processes (Massinai et al., 2023; Song et al., 2011)

At a smaller scale, studies by Triani et al. (2026) and Amelia et al. (2024) used the Wenner configuration to identify weak zones with low resistivity (<100 Ωm), which were interpreted as water-saturated clay layers with low bearing capacity. Amelia et al. (2024) found that these weak zones were concentrated in the topsoil and associated with embankment instability due to subsurface erosion. Similarly, Triani et al. (2026) showed that low-resistivity zones represent vulnerable layers that are susceptible to deformation under changing hydrological conditions. Rizqi and Yudhana (2021) further demonstrated the effectiveness of electrical resistivity methods in detecting subsurface cavities and dissolution features through resistivity contrasts in karst environments. Despite these advances, previous resistivity studies have primarily focused on weak zones, erosion-induced instability, and karst-related cavities. Investigations specifically targeting shallow subsurface conditions around subsurface water channels as potential contributors to localized and recurring land subsidence remain limited. As these features are expected to occur at shallow depths, detailed characterization of near-surface subsurface conditions is required to understand better the mechanisms controlling subsidence development in urban environments.

One important aspect of subsidence concerns the subsurface flow system. In geophysical studies of subsidence, high resistivity values are generally associated with underground voids or air- or water-filled zones, as these materials have greater electrical resistance than the overlying soil (Rizqi and Yudhana, 2021). Conversely, clay or water-saturated materials tend to exhibit low resistivity values due to their water content and conductive properties. This contrast in resistivity serves as the basis for identifying indications of voids, underground channels, or weak zones that may lead to subsidence. Thus, analysis of resistivity patterns can help identify areas at risk of land subsidence. In the context of subsidence in the study area traversed by water channels, the 2D geophysical method is expected to reveal high-resistivity distributions as indicators of subsidence areas and potential for recurring subsidence. Unlike previous studies that primarily focused on

identifying subsidence-prone zones using resistivity data, this study integrates 2D Electrical Resistivity Tomography (ERT), synthetic forward modeling with Res2DMod, and three-dimensional visualization with Leapfrog Geo to investigate recurring land subsidence associated with subsurface water-channel structures. Furthermore, this study evaluates the recurrence of subsidence in a previously repaired area, providing a more comprehensive understanding of the relationships among fill-soil characteristics, groundwater infiltration, subsurface drainage structures, and future subsidence hazards. Therefore, the main scientific contribution of this study lies in integrating geophysical imaging, synthetic modeling, and geological interpretation to assess the risk of recurring subsidence in urban environments. In addition, this study is relevant to physics education because it demonstrates the practical application of electrical resistivity, electric current flow, potential difference, and geophysical inversion concepts to solve real-world environmental and geotechnical problems. Therefore, the results may serve as contextual learning material in physics and geophysics education.

2. METHODS

This study employs a 2D electrical resistivity method to examine patterns of resistivity changes in both vertical and horizontal directions. The application of electrical resistivity is based on Ohm's Law, which states that the potential difference across the ends of a conductor is equal to the product of resistance (R) and current (I). Resistance (R) represents the opposition of a material to electric current flow. Meanwhile, resistivity is a medium's ability to impede the flow of electric current. Resistivity is a material's characteristic of impeding current flow through it. Every material has a different resistivity value. The fluid content and the distribution of metallic minerals within the rock influence the resistivity of the rock beneath the surface (Sastrawan et al., 2020). The geometry factor is a correction factor for differences in the arrangement of current and potential electrodes. Therefore, the value of this geometry factor depends strongly on the measurement configuration used (Santoso, 2016).

In geophysical methods, a current is injected into the subsurface to obtain the apparent resistivity (ρ_a). According to Telford et al. (1990) and Rahmania et al. (2021), the apparent resistivity can be expressed by the following equation.

$$\rho_a = K\frac{\Delta V}{I} \tag{1}$$

where:
ρ_a : Apparent resistivity (Ωm)
K : Geometric factor (m)
ΔV: Potential difference (V)
I : Current (A)

The Wenner-Schlumberger configuration offers relatively good depth penetration, enabling it to better identify variations in resistivity across several subsurface layers than the Wenner configuration with the same path length (Antosia, 2025). This configuration is sufficiently flexible for application in both large and limited survey areas. However, the drawbacks of this configuration include a relatively longer measurement time compared to other configurations and lower sensitivity to horizontal changes (Tjiongnotoputera et al., 2021). Therefore, this configuration is optimal for detecting variations in rock properties with depth (Pambudi et al., 2022). This study employs the Wenner-Schlumberger configuration, which uses a constant-spacing system. In this method, the spacing between potential electrodes is kept constant, while the spacing between current electrodes is gradually varied. This method places the MN potential electrodes at specific intervals, while the AB current electrodes are always moved according to the selected interval (Rizqi and Yudhana, 2021). In this configuration, there is a ratio of the distances between A–M–N–B, where the values of A–M and N–B are each na, while the distance between A–B is a multiple of the spacing a thus, as n increases with depth below the ground surface, the value becomes $2\pi a$ and so on, representing deeper current penetration (Sapina et al., 2023). Additionally, research by Jamaluddin and Umar

(2018) also indicates that the Wenner–Schlumberger configuration is effective for identifying subsurface layers with significant depth penetration. The research stages are described as follows:

2.1 Data Acquisition

Data acquisition involved determining survey lines on a map, laying them out in the field, and conducting geophysical measurements. The survey was carried out over five days in the PATGTL Office area, Bandung. Field conditions during acquisition were generally dry, and the study area is characterized by relatively flat topography. Measurements were performed using an IRIS Instruments SYSCAL Pro SWITCH 72 in the Wenner-Schlumberger configuration on five survey lines, each 52 m long, with 52 electrodes spaced 1 m apart. As part of quality control, electrode positions and contact resistance were checked before acquisition; noisy readings were remeasured, and inversion quality was evaluated using RMS error values. The survey layout is shown in Figure 1.

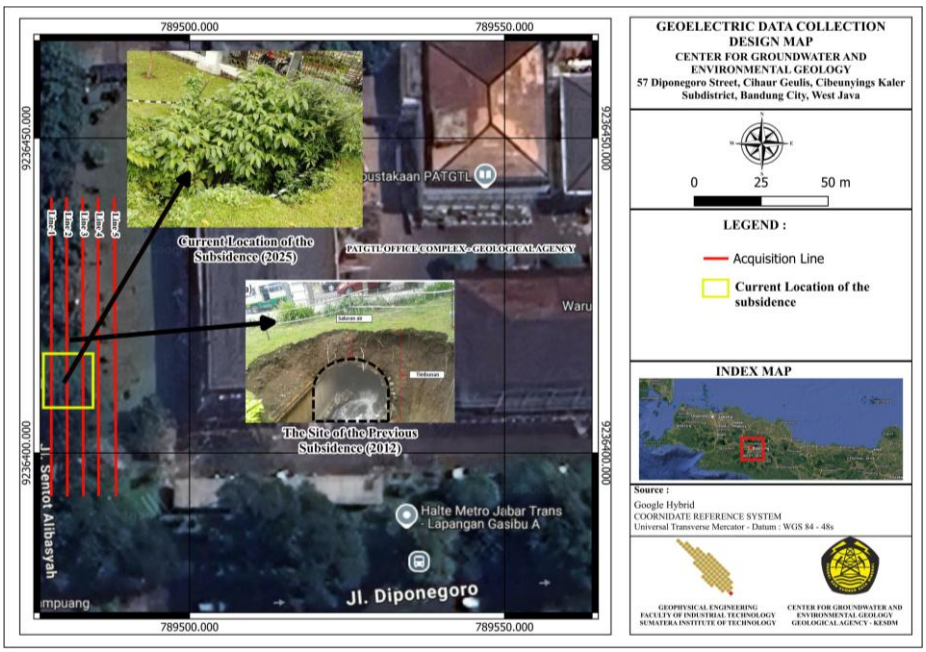


Figure 1. 2D Electrical resistivity survey acquisition design map.

Figure 1 shows a map of the electrical resistivity survey conducted around the PATGTL office complex in Bandung. There are five survey lines marked in red, labeled Line 1 through Line 5, starting from the left. The map also shows the locations of previous subsidence events and the location of the subsidence currently underway. The new subsidence is approximately 3.4 meters deep and has a diameter of 2.7 meters. The length of the measurement line is 52 meters, chosen to accommodate the relatively limited study area. The use of the Wenner-Schlumberger configuration under these conditions is considered appropriate due to its sufficient depth of penetration, even when applied to a relatively small area. Although the survey lines are limited in this study, this configuration still allows for representative depth penetration, with an estimated theoretical penetration depth of approximately 10–13 meters. This depth is expected to be sufficient to provide an understanding of subsurface conditions that could potentially become subsidence zones.

The result of this acquisition process is a set of data points representing subsurface conditions at specific distances and depths. Each data point indicates the position where the apparent resistivity was measured, based on the measured surface current and potential. The distribution of these measured data points is presented as a stacking chart, where the colored points illustrate variations in apparent resistivity. This distribution pattern provides an initial overview of the extent and depth of the investigation prior to the modeling process. Subsequently, the data are processed using the Res2Dinv software via inversion to generate a 2D resistivity cross-section that is easier to interpret, as shown in Figure 2.

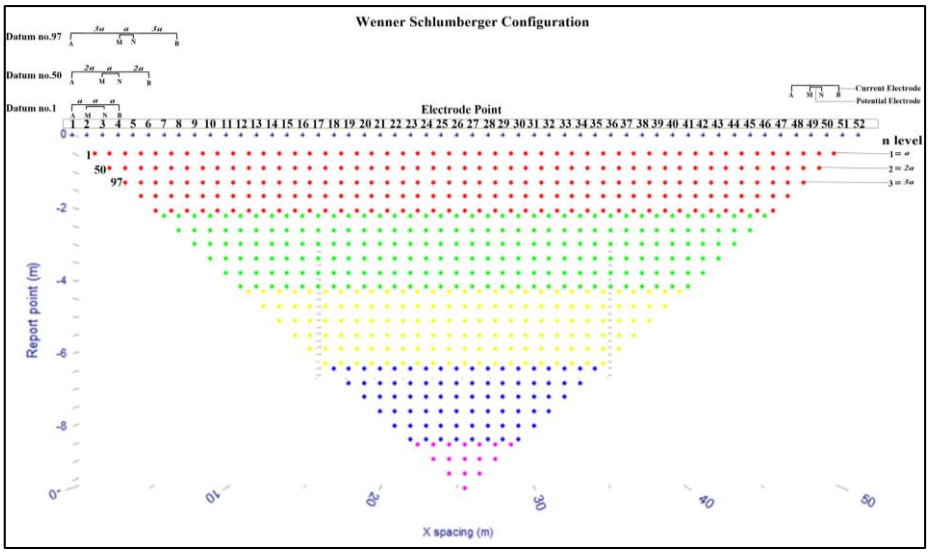


Figure 2. Wenner-Schlumberger stacking chart configuration.

Based on Figure 2, the distribution of measurement points is controlled by the multiplier factor *n*, which determines the depth of investigation. As *n* increases, greater electrode separations result in deeper current penetration into the subsurface. The patterns corresponding to *n* = 1, 2 and 3 are presented as representative examples illustrating the progressive variation in the data distribution with depth. The survey employed the complete Wenner-Schlumberger sequence, and all measurement levels were incorporated into the inversion process, thereby maximizing the investigation depth achieved in this study.

In some areas, points in two distinct colors appear denser or overlapping. This occurs because certain electrode configurations produce measurement points that are geometrically identical or very close together, even though the apparent resistivity values obtained differ. Small variations in subsurface conditions may cause these differences. Additionally, the clustering of data points reflects repeated sensitivity at specific depths, which indirectly increases data density in those zones.

Similarly, the distribution of points from top to bottom of the image illustrates the depth penetration achieved by the measurement configuration. The further down, the data points represent greater depth estimates, although in the modeling results of this survey, the identified effective depth is only about 11.5 meters, which is theoretically controlled by the electrode configuration and the survey line length (Loke et al., 2013). The triangular distribution of points also indicates that the number of points decreases in depth. This suggests that data resolution in the shallow layers is higher than in the deeper layers, allowing surface-layer details to be depicted more clearly. Thus, the data distribution pattern in the figure not only illustrates the depth range and data density but also provides an initial indication that the acquired data is sufficiently representative to support lithological interpretation and the delineation of subsurface layers.

2.2 Data Processing

The measurement data will then be processed and analyzed. The analysis is subsequently modeled in two dimensions using the Res2dinv software with an inversion program. This inversion program also determines the measured and calculated apparent resistivity values (Octavani and Kadri, 2019). The inversion method used in this study is the least squares method. In this 2D electrical resistivity survey, the inversion process is performed on data in DAT format using the least-squares inversion method to obtain a model of the true subsurface resistivity (Yuspancana et al., 2019). The results obtained show variations in the true resistivity (ρ) and RMS Error values. From this data, 2D rock resistivity cross-sections for each measurement line will be obtained based on the contour colors and depths generated (Amelia et al., 2024). Next, synthetic modeling was performed using the Res2Dmod software. Subsequently, the inversion results from each survey line were combined and visualized in three dimensions using Leapfrog Geo, thereby providing a more

comprehensive overview of subsurface resistivity distribution in the study area. The target of the data processing is the true resistivity.

2.3 Synthetic Data Generation

Synthetic data was generated using the Res2Dmod software, where the results of the synthetic geophysical cross-section model closely approximate the actual results. This software divides the model into rectangular blocks and iteratively determines the resistivity of these blocks to accurately reproduce the measured pseudo-resistivity data (Hassan, 2018). In a synthetic model, the true values of the resistivity distribution are known, providing a means to evaluate the quality of the existing inversion results. Therefore, to investigate the reliability and capability of the optimized configuration in identifying geometric structures and reconstructing the resistivity values of various geological features, a synthetic model is essential (Abdullah et al., 2018).

2.4 Data Interpretation

Data interpretation was performed by analyzing variations in inverted resistivity values shown in 2D cross-sections. At this stage, each difference in resistivity values was interpreted as a difference in the physical properties of subsurface materials. Low resistivity values were interpreted as zones of loose, water-saturated, or weathered soil, whereas high resistivity values indicated more compact, relatively stable materials. The 2D profile is then analyzed to identify potential resistivity anomalies associated with subsidence. The presence of localized low-resistivity zones at shallow to intermediate depths, particularly when located beneath the affected area, can be interpreted as weak zones that contribute to subsidence. Based on this resistivity distribution, the potential for subsidence is reassessed in light of the continuity and extent of the low-resistivity zones. If the weak zones are still developing and have not yet shown signs of more compact material, the area remains at risk of recurring subsidence, particularly if affected by changes in load or groundwater conditions.

3. RESULT AND DISCUSSION

The results of the study, based on field data, show the distribution of subsurface resistivity, as illustrated in Figure 3.

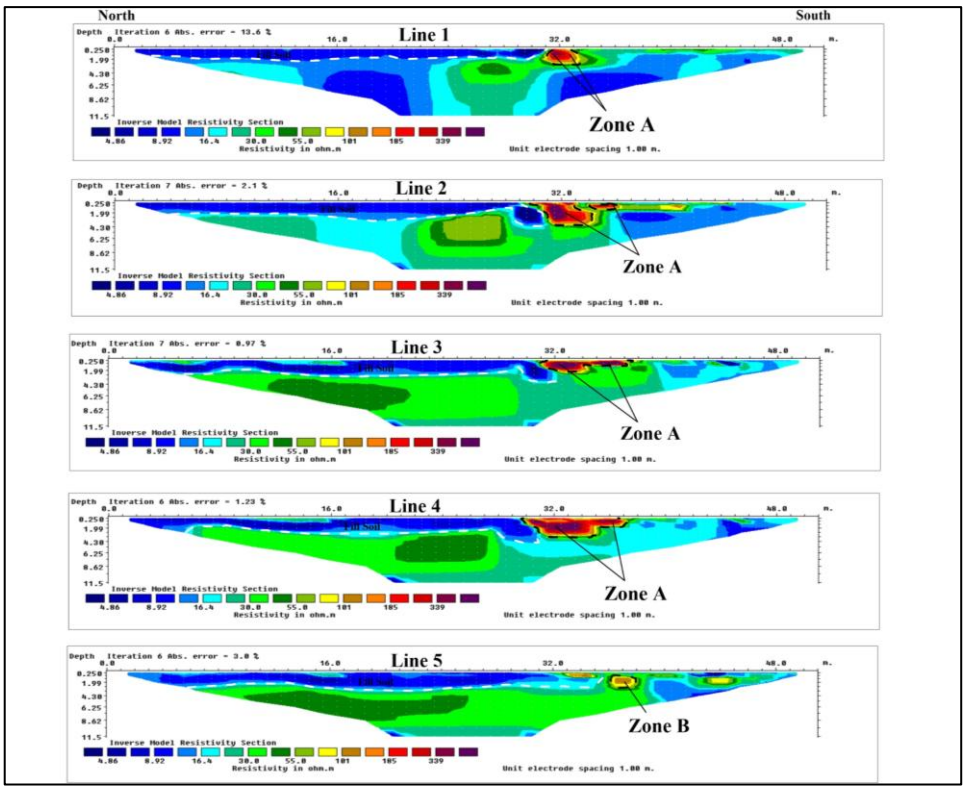


Figure 3. Resistivity cross-section of 5 measurement lines.

Figure 3 shows a 2D electrical resistivity survey in the PATGTL office area, conducted along five transects, each 52 meters long, using the Wenner-Schlumberger configuration. Based on the results of field data inversion, the resistivity cross-sections indicate that the effective depth, which remains well resolved and can be interpreted with sufficient clarity, reaches approximately 11.5 meters across all transects. This indicates that the investigation depth in this study has been achieved in accordance with the field measurement results, and the resulting subsurface model is representative up to that depth limit.

Based on the resistivity cross-sections along the five survey lines, the resistivity values can be classified into three main groups: low, medium, and high. From the surface to shallow depths (0–2 meters), all transects are dominated by a low-resistivity zone indicated by a range of 4.86–16.4 Ωm, shown in blue to light blue. This zone extends for nearly 52 meters along each profile and exhibits a relatively continuous lateral pattern. These low resistivity values indicate materials with high water content and high porosity, which generally represent layers of fill soil or loose surface material (Gunn et al., 2015).

Below the low-resistivity zone lies a moderate-resistivity zone, indicated by a range of 30–55 Ωm and shown in shades of green to greenish-yellow. This zone is more prominent in sections 3, 4, and 5, where it is quite extensive and extends laterally in a relatively continuous manner to intermediate depths. In profiles 1 and 2, zones of moderate resistivity also appear, but their distribution is more limited and intermixed with low-resistivity zones. These moderate resistivity values indicate materials with higher density and compactness than the surface layer, which has a relatively lower water content (Melo et al., 2021). Vertically, this zone generally extends to near the maximum interpreted depth of approximately 11.5 meters.

High-resistivity zones, indicated by values ranging from 101 to 339 Ωm and shown in shades of yellow to red, appear as localized anomalies on several lines. On lines 1 through 4, high-resistivity anomalies are clearly visible in the central to southern parts of the lines at varying depths. Meanwhile, on line 5, high-resistivity anomalies also appear but with more limited dimensions and are located relatively close to the surface. The discontinuous lateral nature of this zone indicates significant changes in the material's physical properties relative to the surrounding environment. High resistivity values indicate drier material, the presence of voids, or the possibility of specific structures that resist the flow of electric current (Seladji et al., 2010). As a result of the forward modeling process, the model results and synthetic data cross-sections are shown in Figure 4 below, representing the subsidence conditions in the field.

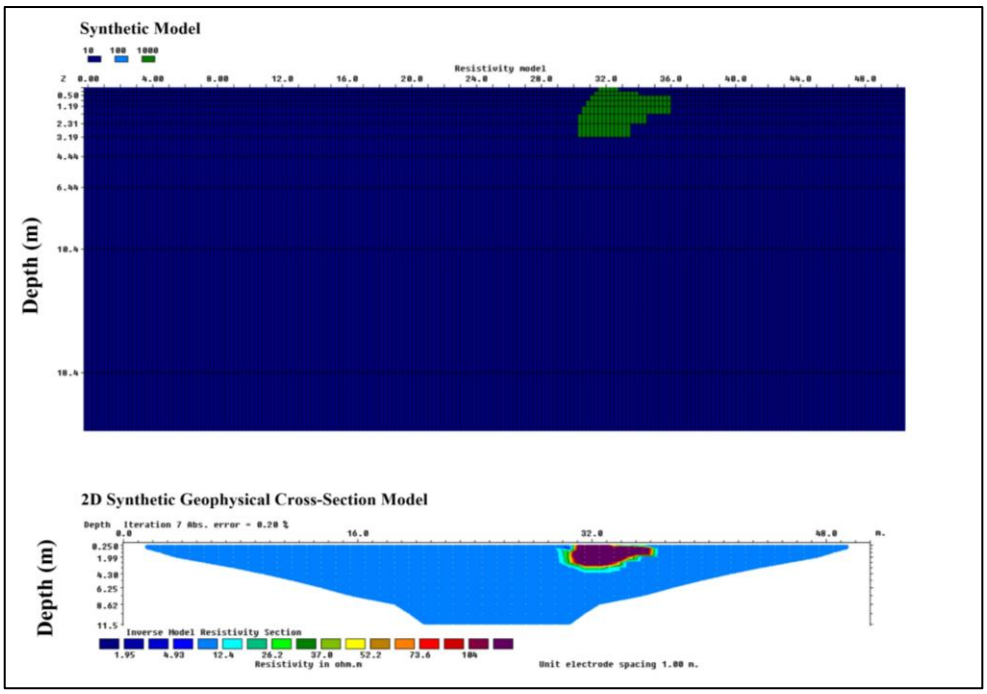


Figure 4. Results of synthetic modeling of subsidence conditions.

Figure 4 shows the results of 2D synthetic geophysical data compiled to represent subsidence conditions at the study site as a conceptual model. This modeling was performed by inputting subsurface geometric and physical property parameters, adjusted based on field observations, so that the resulting model is expected to closely approximate the actual subsidence conditions. The modeling results reveal an anomaly zone with relatively high resistivity values that develops at shallow depths and forms a basin-like pattern. This high-resistivity anomaly, designated as "Zone A", is interpreted as a feature potentially associated with ground subsidence. The observed response may be related to relatively dry conditions, the loss of fine-grained material during subsurface erosion, or the development of localized void spaces. Nevertheless, variations in lithology and material compaction may also contribute to the resistivity contrast. Accordingly, the interpretation is supported by the anomaly geometry, spatial distribution, and consistency with the modeling result rather than by resistivity magnitude alone.

The agreement between the synthetic data models above and the field observation data along Profile 4 is evident geometrically in the shape, position, and dimensions of the high-resistivity anomaly. The synthetic model successfully reproduced the anomaly with a horizontal diameter of approximately 2.7 meters and a maximum depth of 3.4 meters, consistent with the actual subsidence characteristics identified in the field. This indicates that the synthetic model accurately represents the geophysical response to subsidence conditions. The anomaly patterns resulting from the synthetic data inversion process closely resemble those obtained from direct field measurements. This agreement can strengthen the interpretation of field data inversion results and enhance their reliability. Although the synthetic model has shown good agreement, a more detailed geometric representation is needed to describe the physical conditions of the subsurface objects causing the anomalies. Therefore, a sketch of the subsurface water channel network that crosses the study area is shown in Figure 5.

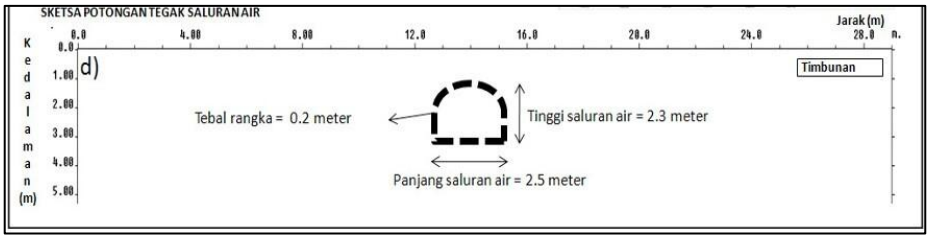


Figure 5. Cross-section sketch of a water channel (Hermawan & Ruchimat, 2019).

The sketch in Figure 5 shows a conceptual cross-sectional model of the subsurface water channel crossing the study area. Geometrically, this channel is semicircular, with a length of approximately 2.5 meters and a height of 2.3 meters, and a relatively thin wall thickness of about 0.2 meters. The channel is located beneath a layer of loose fill soil. Conceptually, these geometric conditions indicate that the cover layer above the water channel is susceptible to ground subsidence, particularly if the fill material has not been adequately compacted. The relatively thin wall thickness also increases the risk of leakage, allowing water to infiltrate the surrounding soil layers.

This interpretation is consistent with previous research by Hermawan and Ruchimat (2019) in the Cikapayang River area, which showed that ground subsidence tends to occur above underground channels due to the weakness of the overlying cover material. Fill material dominated by clay, sandy clay, gravel, and cobble fragments generally has low compaction and high porosity, thereby facilitating water infiltration and reducing soil stability. Furthermore, the presence of water within subsurface channels can be identified by a delay in GPR wave propagation and a reduction in the electric field amplitude. This indicates that water has a significant influence on subsurface physical conditions. Therefore, this study found that water seeping into the backfill soil due to leaks in the thin channel framework can accelerate soil softening and increase the risk of subsidence around the channel.

To correlate the results of water channel sketches from previous studies with the acquired geophysical data, synthetic models were developed, and cross-sections were generated based on the framework sketches and the geometry of the subsurface water channels, as shown in Figure 6.

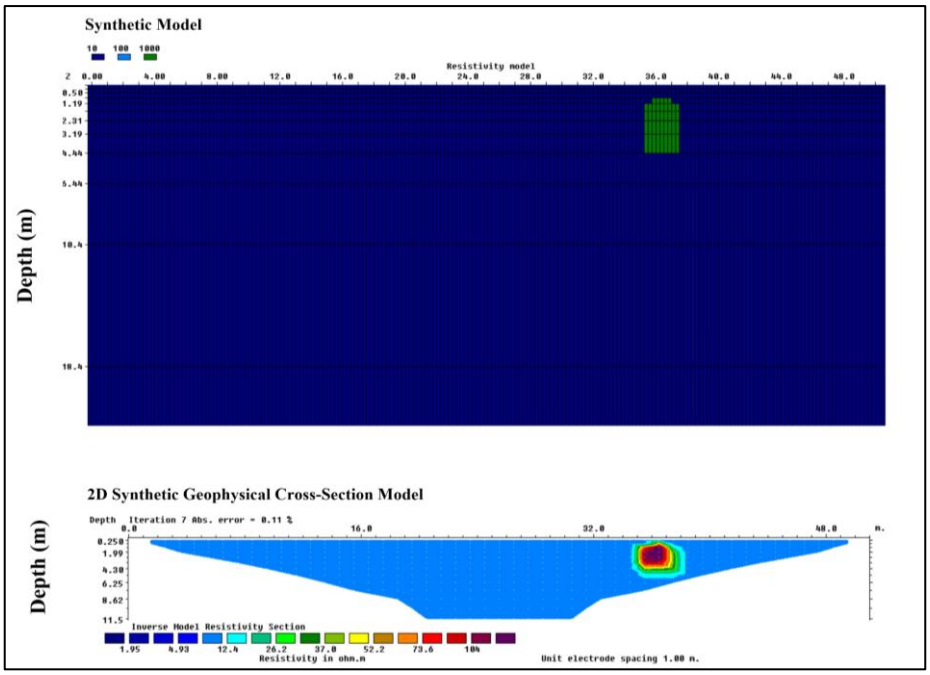


Figure 6. Results of synthetic modeling of a water channel structure.

Figure 6 shows the results of 2D synthetic geophysical data generated based on the framework and geometry of the subsurface water channel. This model was developed by incorporating the dimensions of the water channel that closely approximate actual conditions, namely a semicircular shape with a height of approximately 2.3 meters, a width of 2.5 meters, and a frame thickness of 0.2 meters, located beneath the fill soil layer. In the modeling results, an anomaly zone with relatively high resistivity values is observed at shallow depths, with a lateral position corresponding to the mapped alignment of the water channel shown in the sketch. This feature is designated as "Zone B" and interpreted as a potential subsurface water-channel structure based on its spatial correspondence, geometry, and agreement with synthetic modeling results. The surrounding layers exhibit lower resistivity values, which may be associated with less compact fill material and relatively higher moisture content.

The correlation between the synthetic modeling results and cross-section 5 indicates that the top of the water channel lies approximately 1 meter below ground level. This condition indicates the presence of a relatively thin overburden layer. This layer consists of loose material, making the water channel susceptible to ground subsidence, primarily due to infiltration of water through leaks in the channel's thin walls (Karoui et al., 2018). These conditions align with field observations, in which the water channel was originally covered by fill material before being exposed due to subsidence.

Thus, the forward modeling results and the inversion cross-section not only represent the geophysical response of the synthetic model but also agree well with the geometric sketch of the aquifer. This reinforces the interpretation that the identified resistivity anomalies reflect the subsurface aquifer structure, as depicted in the vertical cross-section sketch. As a result of the forward modeling process, a synthetic cross-sectional data model is shown in Figure 7, representing the conditions in two subsurface layers with different resistivity values.

The results of the synthetic modeling in Figure 7 show subsurface conditions comprising two main layers with contrasting resistivities. The upper layer is characterized by low resistivity (<20 Ωm), while the underlying layer has moderate resistivity (>72.8 Ωm). This two-layer model was developed to represent the soil conditions at the study site, particularly the presence of fill soil as the overlying layer. In the 2D electrical resistivity cross-section inversion results, the same pattern is consistently observed across all measurement profiles. The low-resistivity layer dominates the upper portion, with a relatively uniform thickness along the profiles. This layer is interpreted as fill soil, which is generally composed of loose, not yet well-compacted material and has relatively high water content. These characteristics cause the fill soil to have a lower resistivity than the layer beneath it.

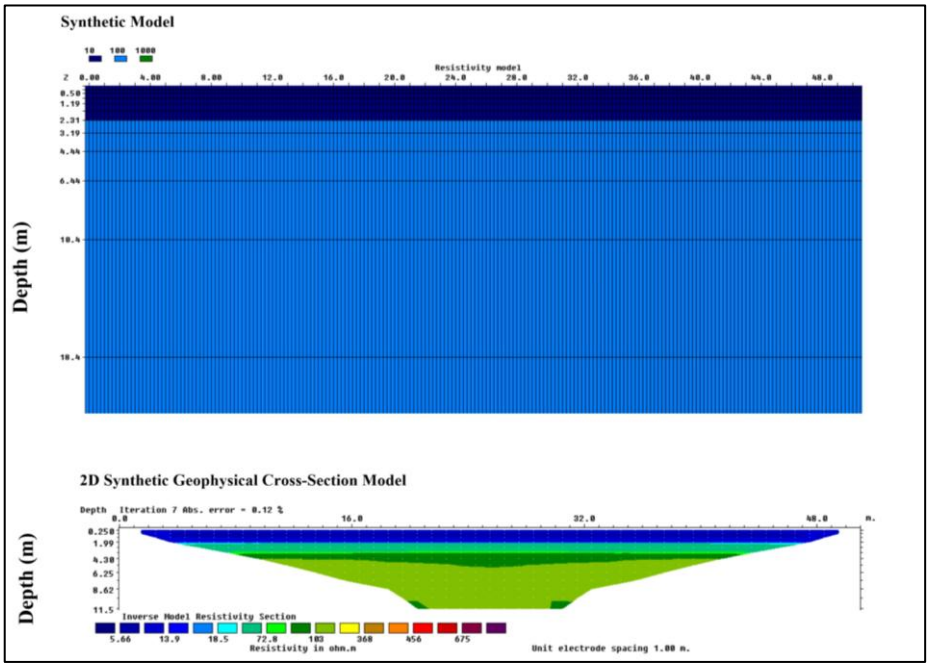


Figure 7. Results of a two-layer synthetic model.

Beneath the fill layer, a layer of moderate resistivity was identified at a relatively consistent depth across all survey lines. This layer is interpreted as a more compact and stable material, which may consist of in-situ soil or constituent material that has undergone greater compaction. The consistency of the resistivity patterns between the synthetic model and the inversion results across all survey lines confirms that subsurface conditions are homogeneous throughout the survey area.

Furthermore, combining the results of each survey line provides a more comprehensive picture of subsurface conditions, particularly the direction and location of water channels in the Cikapayang River. The presence of these subsurface water channels is indicated by zones of high resistivity, shown in red, as illustrated in Figure 8.

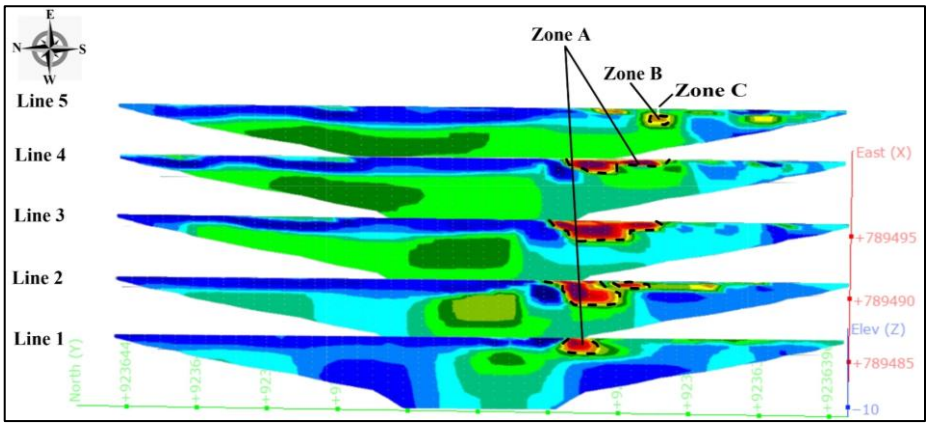


Figure 8. Results of combining all measurement lines.

Figure 8 shows a composite of all geophysical cross-sections from Lines 1 to 5, compiled to provide a comprehensive overview of subsurface conditions in the study area. The combination of survey lines aims to analyze the correlation and continuity of resistivity patterns across the lines, so that the resulting interpretation is not limited to a single line in isolation but more accurately reflects subsurface conditions across the study area. Based on this combined model, layers with low to medium resistivity values dominate the surface and are distributed relatively uniformly across nearly all transects. Referring to the interpretation results from previous studies, this layer is

interpreted as fill soil. Physically, fill soil is generally loose, poorly compacted, and has relatively high porosity and water content. These conditions result in this layer having low bearing capacity, thus potentially causing geotechnical issues if it lies above rigid or non-homogeneous subsurface structures.

Beneath the fill layer, a zone of relatively high resistivity was identified continuously across Lines 1 to 5. The geometry and lateral continuity of this anomaly indicate the presence of a distinct subsurface feature extending throughout the study area. Correlation with synthetic modeling results and interpretation of resistivity sections suggest a possible association with a buried water channel structure. However, elevated resistivity responses may also be influenced by lithological heterogeneity, variations in material compaction, and the relatively dry ground conditions during data acquisition. Previous investigations reported fill material consisting of clay, sandy clay, gravel, and cobble fragments, which may contribute to resistivity contrasts within the subsurface. Therefore, this interpretation is based on the integration of anomaly geometry, spatial continuity, modeling results, and supporting geological information rather than on resistivity magnitude alone.

These findings are consistent with recent studies demonstrating the effectiveness of electrical resistivity tomography in identifying subsidence-prone zones, collapsible soils, and subsurface water channels in urban and geotechnical environments (Jabrane et al., 2023; Meyomesse et al., 2023; Wilopo et al., 2022). Variations in resistivity responses are commonly associated with differences in lithology, moisture conditions, and soil compaction, highlighting the importance of integrating geophysical interpretation with geological and field observations.

Specifically, in “Zone B”, which includes Section 5, relatively higher resistivity values are observed compared to other sections within the same zone. This high-resistivity anomaly, separated from the overlying soil layer, “Zone C”, by a boundary at a depth of approximately 1 meter, is interpreted as a feature associated with a buried drainage channel based on its geometry and spatial distribution. The overlying fill material is characterized by relatively low compaction, which may facilitate rainwater infiltration. An increase in pore-water content can elevate the unit weight of the soil and, in turn, increase the load acting on the underlying layers, thereby increasing the potential for ground subsidence.

Beyond its geotechnical implications, the present study also demonstrates the application of electrical resistivity principles in subsurface investigations. The integration of field measurement, inversion modeling, and geological interpretation provides a practical example of how fundamental physics concepts are applied to analyze real-world environmental problems. Consequently, the findings may serve as contextual learning resources for physics and geophysics education, particularly in topics related to electricity, material properties, and geophysical exploration methods.

4. CONCLUSION

This study successfully identified areas of ground subsidence and potential new subsidence sites around waterways, specifically in the vicinity of the Groundwater and Environmental Geology Headquarters (PATGTL) in Bandung. A 2D electrical resistivity survey using the Wenner-Schlumberger configuration was conducted along five 52-meter-long transects. Inversion results showed resistivity values ranging from 4.86 to 339 Ωm. The low-resistivity zone (4.86–16.4 Ωm) in the shallow layer represents water-saturated, poorly compacted clay fill, which reduces the soil’s bearing capacity. Next is a moderate-resistivity zone with a range of 30–55 Ωm. Meanwhile, high-resistivity anomalies ranging from 101 to 339 Ωm on Lines 1-4 are interpreted as features potentially associated with subsidence zones and subsurface water-channel structures. The interpretation is based on the geometric characteristics and continuity of the anomalies, their agreement with the synthetic modeling results, and direct field observations of existing subsidence features intersected by the survey lines. On profile 5, a zone potentially susceptible to future subsidence was identified at a depth of approximately 1 m, where a relatively thin soil layer overlies an anomaly interpreted as a buried water channel structure. Rainwater infiltration may increase the unit weight of the overlying material, thereby enhancing the load acting on the underlying layer. Synthetic modeling using Res2Dmod and track-merging visualization with Leapfrog Geo verified the consistency of the inversion results with field conditions, including subsidence geometry and water-channel geometry.

These findings demonstrate the effectiveness of the 2D electrical resistivity method for detecting weak zones and subsidence-prone areas in urban environments with fill soil. The research results can serve as a basis for mitigation measures, such as soil compaction control, drainage improvements, and safer infrastructure planning in the PATGTL area.

ACKNOWLEDGEMENTS

We want to express our gratitude to the Center for Groundwater and Environmental Geology (PATGTL) for providing the facilities, equipment, support, and contributions to this research. We would also like to thank our fellow interns from the July–August 2025 internship program at PATGTL for their assistance and cooperation throughout the process, from the preparatory stages of data acquisition to the actual data collection. We hope this research will advance geophysics and serve as a basis for predicting potential new subsidence around the PATGTL area.

REFERENCES

Abdullah, F. M., Loke, M. H., Nawawi, M., & Abdullah, K. (2018). Assessing the reliability and performance of optimized and conventional resistivity arrays for shallow subsurface investigations. *Journal of Applied Geophysics*, *155*, 237–245. https://doi.org/10.1016/j.jappgeo.2018.06.018

Amelia, D., Widyaningrum, Y., & Indriawati, A. (2024). Identifikasi Zona Lemah Tanggul Daerah Aliran Sungai (DAS) Bumang Desa Kemuja Menggunakan Metode Geolistrik Resistivitas Konfigurasi Wenner. *Jurnal Riset Fisika Indonesia*, *5*(1), 29–37. https://doi.org/10.33019/jrfi.v5i1.4940

Antosia, R. M. (2025). A comparative study of vertical geoelectrical arrays in delineating shallow subsurface properties. *Earth Sciences Research Journal*, *29*(1), 81–88. https://doi.org/10.15446/esrj.v29n1.109067

Gunn, D. A., Chambers, J. E., Uhlemann, S., Wilkinson, P. B., Meldrum, P. I., Dijkstra, T. A., Haslam, E., Kirkham, M., Wragg, J., Holyoake, S., Hughes, P. N., Hen-Jones, R., & Glendinning, S. (2015). Moisture monitoring in clay embankments using electrical resistivity tomography. *Construction and Building Materials*, *92*, 82–94. https://doi.org/10.1016/j.conbuildmat.2014.06.007

Hassan, A. A. (2018). Performance of Various Electrical Resistivity Configurations for Detecting Buried Tunnels Using 2D Electrical Resistivity Tomography Modelling. *DJES*, *11*(3), 14–21. https://doi.org/10.24237/djes.2018.11303

Hermawan, W., & Ruchimat, A. (2019). Pemodelan Ground Penetrating Radar Menggunakan Split Step dan Frequency Domain Time Domain (FDTD) Modelling pada Saluran Air Sungai Cikapayang. *Jurnal Lingkungan Dan Bencana Geologi*, *10*(1), 29. https://doi.org/10.34126/jlbg.v10i1.231

Jabrane, O., Martínez-Pagán, P., Martínez-Segura, M. A., Alcalá, F. J., El Azzab, D., Vásconez-Maza, M. D., & Charroud, M. (2023). Integration of Electrical Resistivity Tomography and Seismic Refraction Tomography to Investigate Subsiding Sinkholes in Karst Areas. *Water*, *15*(12), 2192. https://doi.org/10.3390/w15122192

Jamaluddin, & Umar, E. P. (2018). Identification of subsurface layer with Wenner-Schlumberger arrays configuration geoelectrical method. *IOP Conference Series: Earth and Environmental Science*, *118*, 012006. https://doi.org/10.1088/1755-1315/118/1/012006

Karoui, T., Jeong, S.-Y., Jeong, Y.-H., & Kim, D.-S. (2018). Experimental Study of Ground Subsidence Mechanism Caused by Sewer Pipe Cracks. *Applied Sciences*, *8*(5), 679. https://doi.org/10.3390/app8050679

Loke, M. H., Chambers, J. E., Rucker, D. F., Kuras, O., & Wilkinson, P. B. (2013). Recent developments in the direct-current geoelectrical imaging method. *Journal of Applied Geophysics*, *95*, 135–156. https://doi.org/10.1016/j.jappgeo.2013.02.017

Massinai, M. A., Massinai, M. F. I., & Syamsuddin, E. (2023). Land subsidence assessment on karst based on resistivity and geotechnical parameters. *Journal of Degraded and Mining Lands Management*, *10*(2), 4047. https://doi.org/10.15243/jdmlm.2023.102.4047

Melo, L. B. B. de, Silva, B. M., Peixoto, D. S., Chiarini, T. P. A., de Oliveira, G. C., & Curi, N. (2021). Effect of compaction on the relationship between electrical resistivity and soil water content in Oxisol. *Soil and Tillage Research*, *208*, 104876. https://doi.org/10.1016/ j.still.2020.104876

Meyomesse, S. E., Koah Na Lebogo, S. P., Bisso, D., & Zo′o Zame, P. (2023). Application of electrical resistivity tomography and geotechnical techniques for identification and characterization of collapsible soils in Bafoussam (Western, Cameroon). *SN Applied Sciences*, *5*(12), 375. https://doi.org/10.1007/s42452-023-05610-6

Octavani, A. S., & Kadri, M. (2019). Analisis Resistivitas Bawah Permukaan Menggunakan Metode Geolistrik Konfigurasi Wenner–Schlumberger dan Dipole-Dipole di Daerah Geothermal Gunung Sibayak Kabupaten Karo Provinsi Sumatera Utara. *EINSTEIN E-JOURNAL*, *6*(2). https://doi.org/10.24114/einstein.v6i2.12075

Pambudi, R. R., Nurul, M., Prihadita, W. P., & Mulyasari, R. (2022). Comparison of The Electrode Configuration of The Resistivity Geoelectric Method for Landslide Analysis on Highway Suban, Bandar Lampung. *JURNAL GEOCELEBES*. https://doi.org/10.20956/geocelebes.v6i2.17903

Rahmania, Arisalwadi, M., Sastrawan, F. D., & Sari, D. I. (2021). Analyzing of 2D resistivity data to determine the subsurface stratigraphy at Institut Teknologi Kalimantan (ITK) Balikpapan. *Journal of Physics: Conference Series*, *1763*(1), 012014. https://doi.org/10.1088/1742-6596/1763/1/012014

Rizqi, A. H. F., & Yudhana, W. B. M. (2021). Identifikasi Keberadaan Rongga sebagai Pemicu Amblesan (Sinkhole) Berdasarkan Data Geologi dan Geolistrik di Daerah Bedoyo, Kecamatan Ponjong, Kabupaten Gunung Kidul. *Jurnal Mineral, Energi, Dan Lingkungan*, *4*(2), 32. https://doi.org/10.31315/jmel.v4i2.3446

Santoso, B. (2016). Penerapan Metode Geolistrik-2D untuk Identifikasi Amblasan Tanah dan Longsoran di Jalan Tol Semarang – Solo Km 5+400 – Km 5+800. *Spektra: Jurnal Fisika Dan Aplikasinya*, *1*(2), 179–186. https://doi.org/10.21009/SPEKTRA.012.13

Sapina, E., Handayani, L., & Pebralia, J. (2023). Identifikasi Struktur Lapisan Tanah pada Lahan Gambut dengan Metode Resistivitas Konfigurasi Wenner-Schlumberger. *JGE (Jurnal Geofisika Eksplorasi)*, *9*(2), 142–149. https://doi.org/10.23960/jge.v9i2.270

Sastrawan, F. D., Arisalwadi, M., & Rahmania, R. (2020). Identifikasi Lapisan Bawah Permukaan Berdasarkan Data Resistivitas 2 Dimensi. *JST (Jurnal Sains Terapan)*, *6*(2). https://doi.org/10.32487/jst.v6i2.903

Seladji, S., Cosenza, P., Tabbagh, A., Ranger, J., & Richard, G. (2010). The effect of compaction on soil electrical resistivity: a laboratory investigation. *European Journal of Soil Science*, *61*(6), 1043–1055. https://doi.org/10.1111/j.1365-2389.2010.01309.x

Song, S.-H., Lee, G.-S., Um, J.-Y., & Suh, J.-J. (2011). Resistivity Imaging Using Borehole Electrical Resistivity Tomography: A Case of Land Subsidence in Karst Area Due to the Excessive Groundwater Withdrawal. *Journal of the Korean Earth Science Society*, *32*(6), 537–547. https://doi.org/10.5467/JKESS.2011.32.6.537

Telford, W. M., Geldart, L. P., & Sheriff, R. E. (1990). *Applied Geophysics*. Cambridge University Press. https://doi.org/10.1017/CBO9781139167932

Tjiongnotoputera, K. D., Wafi, A., Syarif Setiawan, N., & Mariyanto, M. (2021). Analytical comparison of electrode configuration on 2D geoelectric method for identification of water seepage in the lake body. *Journal of Physics: Conference Series*, *1825*(1), 012019. https://doi.org/10.1088/1742-6596/1825/1/012019

Triani, T., Kamur, S., & Erfina, E. (2026). Aplikasi Metode Geolistrik Resistivitas untuk Menentukan Zona Lemah (Studi Kasus: Wilayah Episenter Gempabumi di Kecamatan Lalolae, Kabupaten Kolaka Timur). *Jurnal Fisika Unand*, *15*(1), 49–56. https://doi.org/10.25077/jfu.15.1.49-56.2026

Wahyudi, E. J., Hafidza, M. H., & Tahta, M. A. (2021). Simple design to estimate time-lapse microgravity response due to shallow subsurface density redistribution caused by land

subsidence. *IOP Conference Series: Earth and Environmental Science*, *873*(1), 012040. https://doi.org/10.1088/1755-1315/873/1/012040

Widada, S., Zainuri, M., Yulianto, G., Satriadi, A., & Wijaya, Y. (2020). Estimation of Land Subsidence Using Sentinel Image Analysis and Its Relation to Subsurface Lithology Based on Resistivity Data in the Coastal Area of Semarang City, Indonesia. *Journal of Ecological Engineering*, *21*(8), 47–56. https://doi.org/10.12911/22998993/127394

Wilopo, W., Putra, D. P. E., Fathani, T. F., Widodo, S., Pratama, G. N. I. P., Nugroho, M. S., & Prihadi, W. R. (2022). Identification of subsidence hazard zone by integrating engineering geological mapping and electrical resistivity tomography in Gunung Kidul karst area, Indonesia. *Journal of Degraded and Mining Lands Management*, *9*(2), 3281–3291. https://doi.org/10.15243/jdmlm.2022.092.3281

Yuspancana, B. D., Purwanto, M. S., Bahri, A. S., & Utama, W. (2019). Integrasi Data Resistivitas 2D Dengan Parameter Fisis Dan Mekanis Tanah Untuk Evaluasi Daya Dukung Tanah (Studi Kasus : Ruas Jalan Kawasan Jiipe, Manyar, Gresik). *Jurnal Geosaintek*, *5*(2), 84. https://doi.org/10.12962/j25023659.v5i2.5403

Zhao, X., Yang, B., Yuan, S., Shen, Z., & Feng, D. (2022). Seepage–Fractal Model of Embankment Soil and Its Application. *Fractal and Fractional*, *6*(5), 277. https://doi.org/10.3390/fractalfract6050277